Application of chiral bi- and tetra-dentate bispidine-derived ligands in the Copper (II)-catalyzed asymmetric Henry reaction

Arianna Rossetti,[a] Stefano Landoni,[a,b] Fiorella Meneghetti,[*b] Carlo Castellano,[c] Matteo Mori,[b] Greta Colombo Dugoni[a] and Alessandro Sacchetti[*a]

The application of a number of chiral bispidine-based ligands in the copper-catalyzed enantioselective Henry reaction is here reported. Results showed good conversion rates and low to moderate enantiomeric ratios, depending on the substituents on the bispidine core. Enantioselectivities of selected ligands were rationalized on the basis of single-crystal X-ray analyses, NMR studies and computational tools.

Introduction

Reactions involving the formation of a new C-C bond are the most valuable and interesting in organic synthesis. One of the most common approaches is to exploit the reaction between a carbanion and an electrophilic carbon. The Henry reaction, also known as nitroaldol reaction,[1] refers to the addition of a nitroalkane anion on a carbonyl carbon to afford a β-nitro alcohol. These compounds are of great interest as intermediates for the synthesis of different products after the transformation of either the nitro or the hydroxyl function.[2] In the past years, many efforts have been made to achieve high enantioselection in these reactions, and a lot of chiral metal catalysts have been proposed.[3] More recently, organocatalytic methods have shown to be very effective in affording nitroalcohol adducts, in high yields and excellent enantiomeric excesses.[4] In the last years, the usefulness of chiral bispidines as ligands in many metal-catalyzed reactions has been demonstrated. Chiral bispidines were initially proposed as surrogates of (-)-sparteine, a natural alkaloid which has been successfully employed as a ligand in the addition of lithium carbanions to several electrophiles. Bispidines can often be easily prepared in one pot and they have been shown to be more versatile as ligands compared to (-)-sparteine, being effective in a wide range of applications[5] and enantioselective transformations.[6] The use of a dichloro[(-)-sparteine-*N*,*N'*]copper(II) complex as a catalyst[7] and of a tricyclic sparteine surrogate[8] were reported in the addition of nitromethane to various aldehydes with moderate to good enantiomeric excesses. More recently, a tricyclic bispidine-based ligand was efficiently applied in the same reaction.[9] On this basis, we decided to employ some chiral bispidines as ligands for the same reactions.

Following our recent interest in the conformational behavior of chiral bispidines,[10] we decided to investigate new potential applications of chiral bispidines in the nitroaldol additions in order to explore the enantioselection in connection with the ligand asymmetry. Therefore, we prepared and screened a library of heterogeneous bispidine ligands in the reaction of nitromethane with aldehydes, under different conditions with diverse metals. The mode of chelation of selected ligands was further investigated by NMR and supported by crystallographic data and computational study to assess the role of the ligand in the stereochemical outcome of the reaction.

Results and Discussion

The synthesis of the bispidine moiety is straightforward and allows the preparation of structurally diverse ligands. Unsymmetrical bispidines **1a-c**[6e] (Scheme 1) were prepared through a multicomponent Mannich reaction between *N*-methyl-4-oxo piperidine and a chiral primary amine in the presence of two equivalents of formaldehyde, under acid catalysis. In this case, a C_1-symmetric ligand, lacking any symmetry elements, is obtained. The C_2-symmetric ligands **2a-c**[6e] were synthesized with a similar approach (Scheme 2), through a one-pot quadruple Mannich reaction, starting from 1,3-diphenyl acetone, four equivalents of formaldehyde and two equivalents of the chiral primary amine. Finally, α-aryl substituted bispidines **4a-c**[10] were prepared by a two-steps procedure (Scheme 3): the reaction of dimethyl-3-oxoglutarate with an aromatic aldehyde and methylamine afforded the intermediates **3a,b**, which were then reacted with formaldehyde and the chiral primary amine to yield products **4a-c**. With this procedure, it was possible to introduce more electron-donating atoms in the scaffolds, thus obtaining a tetra- (**4b**) and a penta- (**4c**) coordinating ligands.

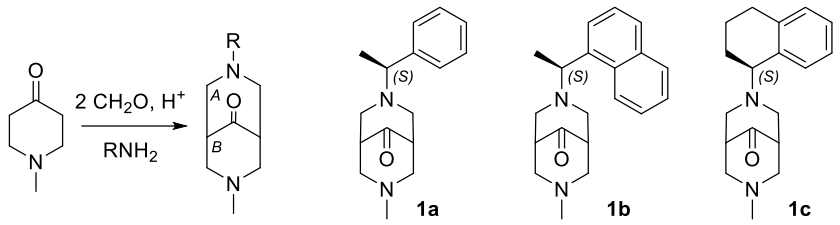

Scheme 1. Synthesis of bispidines **1a-c**.

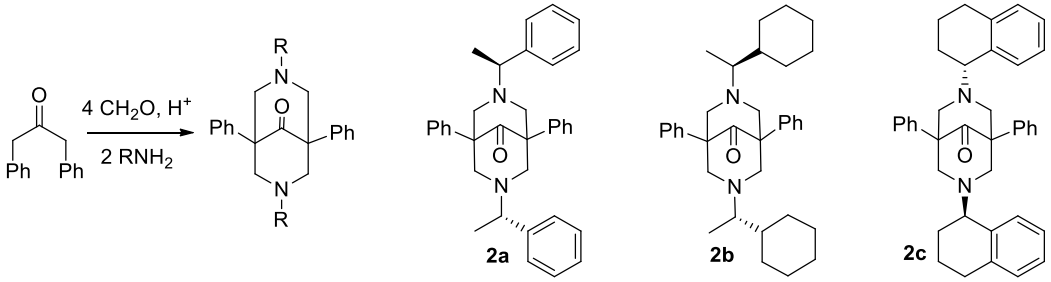

Scheme 2. Synthesis of bispidines **2a-c**.

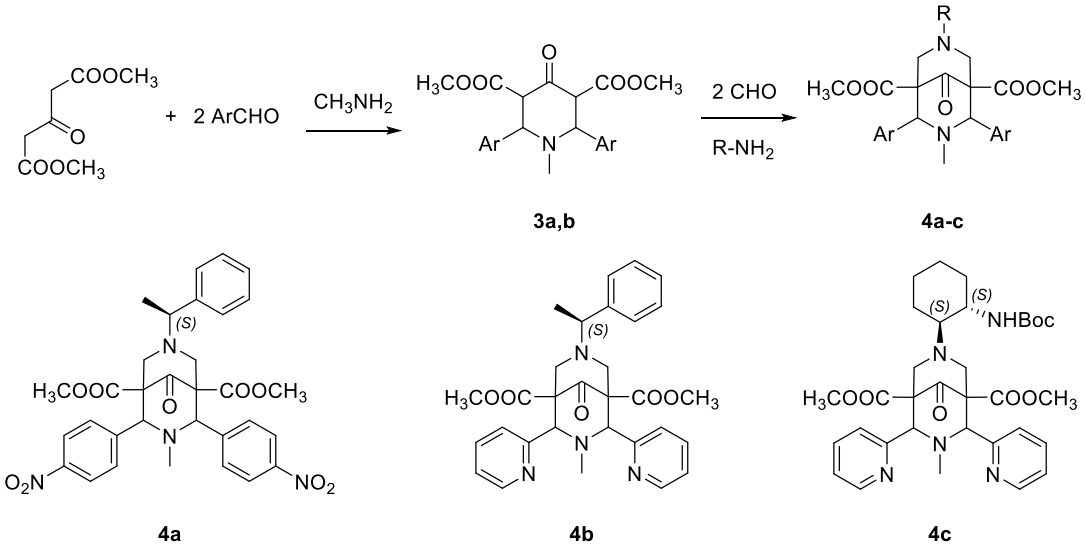

Scheme 3. Synthesis of bispidines **4a-c.**

The copper(II)-catalyzed reaction between nitromethane and benzaldehyde with ligand **1a** was selected for optimizing the reaction conditions. In order to have an easier reaction setup, the ligand-metal complex was pre-formed *in situ* without the need of isolation, starting from copper acetate as the metal source. The nitromethane/benzaldehyde ratio was 10:1, and reactions were carried out at room temperature, without the use of inert atmosphere, for 24 hours. In a first attempt, the use of 10% mol of the complex resulted in a poor 57/43 er and a 31% yield (Table 1, entry 1). The use of the isolated pre-formed complex between ligand **1a** and $Cu(OAc)_2$ showed no remarkable differences compared to the *in situ* generation of the catalyst (entry 2). We envisaged that the presence of an external base would be helpful, in order to assist the deprotonation of nitromethane; therefore, we added a catalytic amount of triethylamine (entry 3), thus obtaining a good yield, but still a moderate enantioselection (61/39 er). When an excess of ligand was used as a base, the er raised up to 70/30 (entry 4), which emphasized the role of the deprotonation step in the catalytic process. Decreasing the temperature did not improve the enantioselection and lowered the yield (entry 5). A solvent screening showed that an alcoholic solvent was necessary, since apolar ones were effective but gave low er. Strongly polar solvent, instead, like DMSO or even water (entry 6,7) were detrimental for the catalytic process, leading to a loss of enantioselection. We could explain this result by assuming a strong coordination between the solvent and the copper atom, which can disrupt the chiral complex by displacing the ligand and ultimately producing no enantioselection. The employment of both THF and chloroform led to increased reaction yields, but still low values of er were detected (entry 8,9). The same happened with the use of neat nitromethane, which dramatically reduced the selectivity of the catalyst, affording a 55/45 er (entry 10). The employment of the salt $CuCl_2$ (entry 11) as the metal source was detrimental, probably due to its lower solubility in the solvent of choice, compared to $Cu(OAc)_2$; therefore, it resulted less efficient in generating the catalytic complex. Finally, we investigated the use of zinc-based catalysts. In this case, lower yields and er were obtained both with $ZnCl_2$ and $Zn(OAc)_2$ (entry 12 and 13).

Table 1. Screening of reaction conditions.

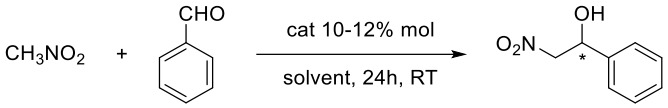

Entry	Solvent	Metal salt (10% mol)	Ligand mol (%)	Yield (%)	er
1	EtOH	$Cu(OAc)_2$	10	31	57/43
2[a]	EtOH	$Cu(OAc)_2$	10	44	59/41
3[b]	EtOH	$Cu(OAc)_2$	10	91	61/39
4	EtOH	$Cu(OAc)_2$	12	90	70/30
5[c]	EtOH	$Cu(OAc)_2$	12	83	70/30
6	DMSO	$Cu(OAc)_2$	12	45	0[d]
7	H_2O	$Cu(OAc)_2$	12	33	0[d]
8	THF	$Cu(OAc)_2$	12	88	59/41
9	$CHCl_3$	$Cu(OAc)_2$	12	71	64/36
10	CH_3NO_2	$Cu(OAc)_2$	12	89	55/45[d]
11	EtOH	$CuCl_2$	12	65	69/31
12	EtOH	$ZnCl_2$	12	59	60/40
13	EtOH	$Zn(OAc)_2$	12	78	67/33

[a] preformed isolated complex was used. [b] 0.2 equiv. of TEA were added. [c] reaction at T = 0°C. [d] probably resulting from the uncatalyzed background reaction.

As a consequence of this screening, we were able to identify the best reaction conditions: the catalyst was generated *in situ* by mixing 0.1 mmol of $Cu(OAc)_2$ and 0.12 mmol of the ligand in ethanol (5 mL was found to be the right amount). Neither inert atmosphere nor dry solvents were required. After stirring the complex at room temperature for 30 min, 1 mmol of aldehyde was added, followed by 10 mmol of nitromethane. After 24 hours, the reaction was complete. With this set of reaction conditions, all the ligands were screened in the Henry reaction with benzaldehyde. Results are reported in Table 2.

Table 2. Screening of the ligands in the Henry reaction with benzaldehyde.

Entry	Ligand	Yield (%)	er
1	**1a**	78	70/30
2	**1b**	71	76/24
3	**1c**	64	68/32
4	**2a**	66	51/49
5	**2b**	59	50/50
6	**2c**	65	52/48
7	**4a**	5	50/50
8	**4b**	92	57/43
9	**4c**	5	50/50

With C_1-symmetric ligands **1a-c**, we obtained overall good yields, and the highest er was achieved with ligand **1b** (Table 2, entry 2). C_2-symmetry ligands **2a-c** were also effective in producing the nitroaldol adduct, but no enantioselection was obtained. An increased steric hindrance in ligand **4a** caused a dramatic drop in yields, as in the case of the pentadentate ligand **4c**. With C_1-symmetric tetracoordinating ligand **4b**, instead, again good yields were obtained, but a very low er was measured in this case too. These results suggest that with **4c** the metal atom is fully coordinated and is therefore not able to interact with the reagents, whereas with **4b** the copper atom has still at least one free coordination site for activating the aldehyde, thus promoting the addition reaction.

In order to further explore the effectiveness of the catalyst, the best performing ligands **1b** and **4b** were employed in the Henry reaction with different aromatic and aliphatic aldehydes (Table 3). Fair to good conversions were achieved with all aldehydes. With aromatic substrates, an er up to 83/17 was obtained (Table 3, entry 3), whereas with aliphatic aldehydes no enantioselection was observed.

Table 3. Screening of aldehydes in the Henry reaction with ligands **1b** and **4b**

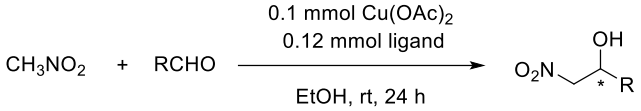

Entry	Aldehyde (R-CHO)	Yield (%)		er	
		1b	**4b**	**1b**	**4b**
1	PhCHO	89	71	76/24	55/45
2	*p*-Br-PhCHO	93	70	78/22	60/40
3	*p*-F-PhCHO	92	74	83/17	53/47
4	*p*-CF_3-PhCHO	93	81	63/37	55/45
5	*o*-NO_2-PhCHO	48	56	55/45	50/50
6	2-naphtaldehyde	79	81	87/13	56/44
7	isovaleraldehyde	65	44	50/50	50/50
8	butyraldehyde	44	39	50/50	50/50

To rationalize the behaviour of the ligands, we studied the structural features of some of the synthesized bispidines by means of spectroscopic and computational tools. Ligands **1a-b** and **4b** had been previously investigated by our group.[10] In particular, single crystal X-ray structures of **1b** and **4b** were determined (Scheme 1), providing useful information on the spatial arrangement of the chiral *N*-naphthylethyl (**1b**) and *N*-phenylethyl residues (**4b**) with respect to the bispidine core, which influenced the chiral space around the metal-chelating center.

We demonstrated that the introduction of large substituents on the nitrogen, as in **1b**, promotes a boat conformation of the piperidine ring, whereas with aromatic substituents on the α position, a chair-chair conformation is preferred. As the stereochemistry of these molecules is a major determinant of their properties, we unambiguously established the absolute structure of the newly synthesized compounds **2a** and **4a**, by X-ray analyses.

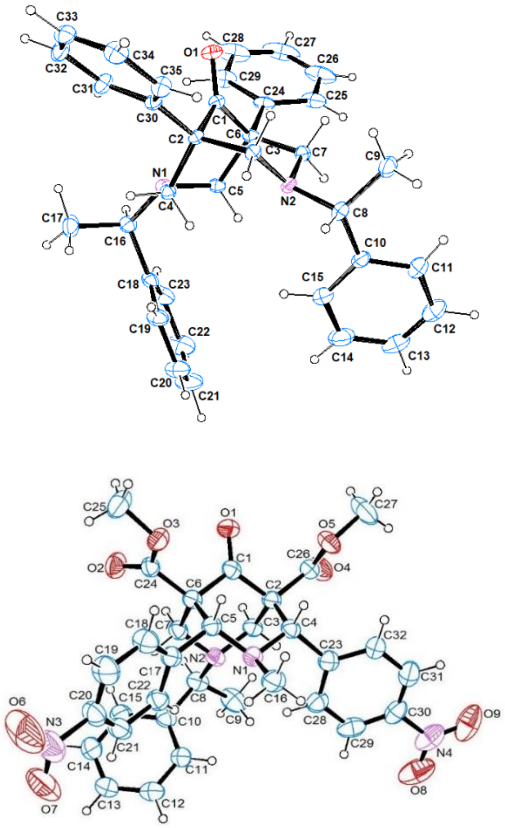

Figure 1. ORTEP drawing[12] of **2a** (above) and **4a** (below) with the arbitrary atom numbering scheme (ellipsoids are at 40% probability).

In accordance with our previous observations,[10] derivative **2a** (Figure 1) showed a boat-chair conformation with the phenyl rings of the chiral residues in an *endo* position. One ring is in chair conformation as shown by the puckering parameters:[12] QT = 0.673(3) Å, ϕ = -148(3)° and ϑ = 173(2)°. On the other hand, the additional ring adopts a boat conformation and the puckering parameters are: QT= 0.7825(3) Å, ϕ = -4.2(2)° e ϑ = 92.0(1)°. The phenyl rings C30-C35 and C24-C29 are inclined with respect to each other with a dihedral angle of 50.4(2)°, while C24-C29 and C18-C23 rings form a dihedral angle of 61.8(2)°. C30-C35 and C18-C23 rings are oriented at 46.2(1)°; C24-C29 and C10-C15, C18-C23 and C10-C15 rings are almost perpendicularly disposed (dihedral angles of 89.2(2)° and 82.5(1)°, respectively).

The crystal structure of **4a** showed that the unit cell contained large accessible voids, where there was no evidence of included solvent. Despite the low quality of the crystals, the structure determination of **4a** provided incontrovertible results of the chair-chair conformation of the bispidinone scaffold, differently from what observed for the solid state structure of **2a** (Fig. 1). For ring C1/C2/C4/N1/C5/C6, the puckering parameters[11] are: Q_T = 0.591(4) Å, ϕ = -36.9(2)° and ϑ = 7.2(3)°, and for the other ring of the bispidine-core they are Q_T= 0.612(8) Å, ϕ = -156.4(2)° e ϑ = 170.8(1)°. The phenyl C23/C32/C31/C30/C29/C28, C10-C15, C17-C22 rings are inclined by 30.4(1)°, 38.6(1)° and 33.0(1)° with respect to the chair A (see scheme 1) mean plane. Moreover, they are almost perpendicular to the chair B mean plane (dihedral angles of 89.8(1)°, 88.5(1)° and 89.5(1)°). The C23/C32/C31/C30/C29/C28 and C10-C15 rings are oriented at a dihedral angle of 58.4(1)° with respect to each other. C10-C15 and C17-C22 rings form a dihedral angle of 77.6(2)°, while C23/C32/C31/C30/C29/C28 is inclined by 38.7(1)° with respect to ring C17-C22.

The different conformation of the bispidine core in **2a** and **4a** confirmed the ability of this scaffold to easily switch from a close (chair-chair) to an open (chair-boat) conformation. This flexibility is important to promote an efficient coordination of the metal in view of their application as catalysts.

In both **2a** and **4a**, the crystal packing is consolidated by Cπ-H···O type intermolecular interactions (see Supporting Information). It is important to point out that in the crystal structures of both compounds the intermolecular contacts do not influence the conformation of the bicycle, as the aromatic moieties are not involved in stacking interactions.

Further information on the preferred conformation in solution could be gathered form ^{1}H-NMR. In particular, the equatorial hydrogens of **2b,c** displayed a small coupling constant ($J \leq 1$Hz) as a consequence of long-range W-coupling along the H-C-N-C-H chain. This observation supported the chair-chair conformation as the preferred one in solution.

For the sake of comparison, ligands **2a** and **4a** were also investigated by computational tools. Moreover, these latter allowed us to gather further information about the conformational behaviour of the ligands. After a conformational analysis (Monte Carlo search with Molecular Mechanics energy minimization), the most favourable conformers were submitted to DFT-B3LYP/6-31G(d) energy optimization *in vacuo* (Figure 2). After the frequency calculation, the energies were corrected by ZPE

addition. For ligand **2a**, we considered both the chair-chair and the boat-chair conformations as possible, in accordance with the findings from solid state. The structure provided with the lowest energy is in the boat-chair conformation, in accordance with the solid state result, while the first chair-chair conformer is found to be 2.48 kcal/mol higher in energy. As for **4a**, three conformers were identified, corresponding to the three different rotamers of the chiral residue. The lowest energy conformer has the methyl group placed in the *endo* position of the bispidine core: the others are very similar in energy, so we could assume that all these conformers are almost equally distributed.

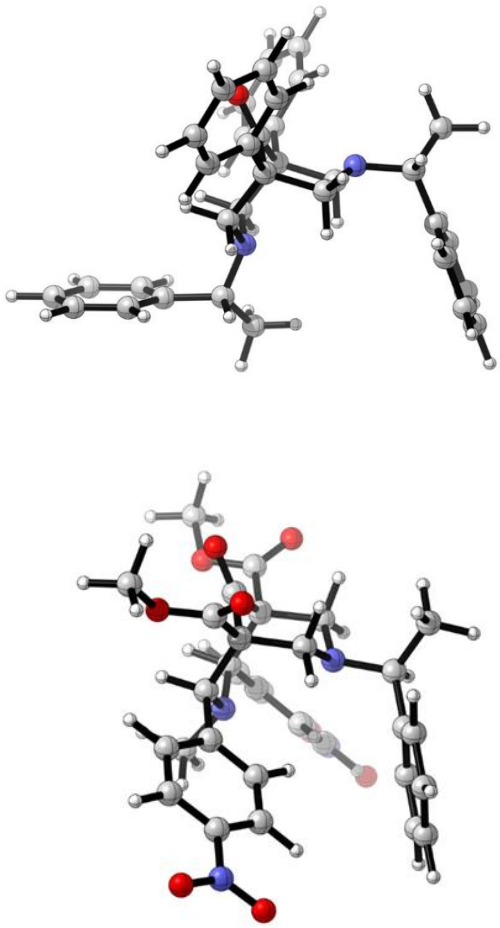

Figure 2. Plot of the energy minimum as obtained for DFT calculations for **2a** (above) and **4a** (below).

The coordination chemistry of ligands **1b**, **2a** and **4a,b** was then further investigated by NMR titration studies, to gather information on the possible complexes formed in solution. To allow the recording of NMR spectra, Zn(II) was used instead of the paramagnetic Cu(II) ion. Ligands were dissolved in $CDCl_3$ and then titrated with a CD_3OD solution of hexahydrated zinc nitrate, starting from 0.25 up to 2 equivalents of metal. During the addition of zinc nitrate to the ligand **4b**, we observed the formation of a new single species **4b'** (Figure 3). After the addition of 1 eq. of metal, the free ligand completely disappeared and only **4b'** was present. Most of the NMR signals moved downfield as a result of the deshielding effect of the metal cation.[11] All the bispidine core hydrogens were shifted, and, as expected, so were the hydrogens adjacent to the pyridine nitrogen coordinating the metal. Since in the free ligand the pyridine nitrogens are oriented in an *exo* position, the metal coordination resulted in a rotation of the pyridine ring toward the *endo* position, further demonstrating the conformational flexibility of the bispidine. When one more equivalent of metal was added, no significant changes were observed. The simultaneous decrease in intensity of the peaks of the free ligand and the growth of the ones belonging to the complex indicated tight binding conditions, resulting in a slow exchange process, in which two defined species are observed, the free ligand and the 1:1 metal/ligand complex.

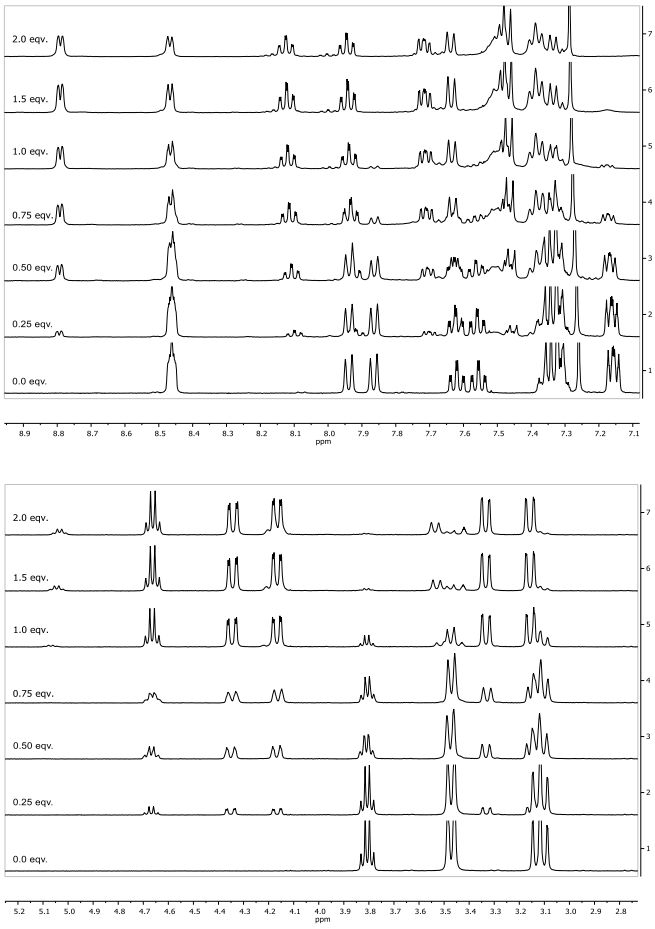

Figure 3. NMR titration spectra for ligand **4b** (above, aromatic region) and **2a** (below, aliphatic region).

A similar result was obtained with bispidine **2a** (Figure 3). The spectrum showed half a set of signals, indicating that a single new C_2-symmetric species is formed, in which the bispidine is coordinating the metal in a chair-chair conformation. The equatorial and the CH hydrogens are the most deshielded (up to 1 ppm), whereas little changes are observed in the aromatic region. This could suggest an *exo* position of the aromatic ring of the chiral residue, which could explain the absence of enantioselectivity for this ligand. Again, if compared with the boat-chair conformation observed in the solid state, we can infer that the bispidine can easily switch to the chair-chair conformation in solution. In this case, the addition of more than 1 equivalent of metal produced the formation of a small amount (ca. 20%) of a new species. A very different situation was observed for ligand **1b**. In this case, after the addition of the first aliquot of metal, two new species appeared in a 3:1 ratio. More significantly, the signals were broadened and no multiplicity could be clearly detected. During the titration, the chemical shifts also changed. This behaviour is typical of a poor binding which produces different species in a fast exchange process. Lastly, when ligand **4a** was titrated under the same conditions as previously described, no significant change in the spectra was observed even after the addition of two equivalents of the cation. In this case, the inner space of the bispidine core is hindered by the presence of the aromatic hydrogens of the *p*-nitrophenyl group, thus precluding the coordination of the metal (whereas for ligand **4b,c** the presence of the pyridine nitrogen promoted the complexation). Lastly, for ligand **4c** an intermediate behaviour was observed. After the first additions of the metal, new broad signals appeared resulting in a not clear spectrum. When one equivalent of metal was added, a new major species emerged with signals sharp enough to make the spectrum clear again. All the signals resulted shifted under the effect of the metal cation; remarkably, also the cyclohexyl hydrogen atoms and the *t*-Bu group resulted to be shifted, suggesting that the Boc carbamate nitrogen could also be involved in the complexation of the metal. In order to examine in depth the coordination-mode, we also attempted to obtain single crystals of the bispidine/copper complexes, unfortunately without success, but for the racemic form of **4b**, which reacted with copper chloride to afford the **4b-CuCl** complex. Crystals suitable for X-ray analysis were obtained from 1:1 EtOH/water solutions, as light blue platelets (Figure 4). Despite the low quality of the crystal of **4b-CuCl**, mainly due to the resolved and unresolved disorder, this X-ray study provided concrete knowledge about the coordination around the copper ion and confirmed the required chair-chair conformation of the bispidinone scaffold for complexing the metal.

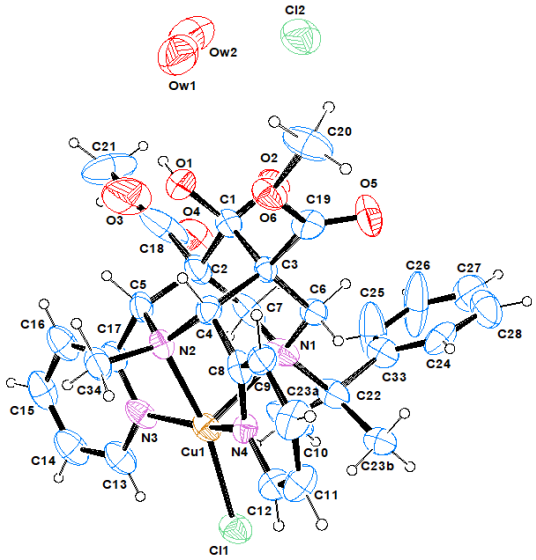

Figure 4. ORTEP drawing[13] of **4b-CuCl** with the arbitrary atom numbering (ellipsoids are at 40% probability and H atoms are as spheres of arbitrary radii). The phenylethyl residue in the asymmetric unit is equally disordered over two sites.

Compound **4b-CuCl** crystallizes in the monoclinic system, in the centrosymmetric space group $P2_1/c$. ORTEP[13] drawing in Figure 4 shows the coordination geometry around the metal center and the disorder present in the crystal structure on the *N*-phenylethyl residue, due to the presence of both the enantiomers at the stereogenic center C22. Indeed, the methyl group linked to this asymmetric carbon atom exists in the solid state in two different conformations, disordered over two sites (50% probability). Inspection of the positions of the two alternative orientations of the residue linked to N1 evidenced that the two arrangements are related by inversion of the carbon stereochemistry, indicating that the two different forms are a consequence of the simultaneous occurrence of two diastereoisomers at the same crystallographic site. In addition to the copper complex, the asymmetric unit

comprises also a chlorine anion and two water molecules, which joined into supramolecular one-dimensional chains. The presence of a high degree of molecular disorder in this crystal structure, may account for the poor quality of the crystals and the difficulties in achieving samples suitable for X-ray analysis. This condition is frequently observed in this kind of coordination complexes.[14]

Usually, in the copper(II) complexes where the distortion of the coordination polyhedron is dominated by the Jahn-Teller effect, we should expect four closer planar donors (with Cu-O or Cu-N bond of ca. 2 Å) and one or two axial/distal longer bonds. In this complex, the Cu atom is pentacoordinated (Figure 5), linking two N atoms of the bispidine ligand, two N atoms of the chelating pyridine rings, and a Cl atom. The axial position is occupied by the N1 of the bicycle. Bond lengths and angles are in agreement with literature data.[15] The deviation of the Cu(II) atom from the mean plane composed of atoms N2, N3, N4 and Cl1 is 0.259(1) Å.

According to Addison and co-workers, for distorted pentacoordinated structures, the parameter θ (θ = (β-α)/60°), where α and β are the largest angles around the metal centre, can be used to rationalize their geometries. The value of θ is 0 for perfectly square-pyramidal geometries and 1 for perfectly trigonal–bipyramidal geometries. With regard to **4b-CuCl**, θ is about 0.19, suggesting a slightly distorted square–pyramidal conformation.

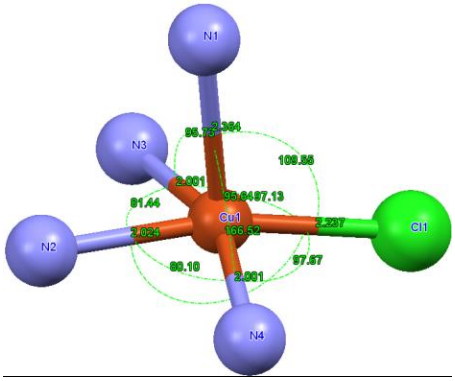

Figure 5: Coordination sphere of **4b-CuCl**: distances and angles.

In the complex, the bicyclo[3.3.1]nonane ring adopts a chair-chair conformation. The puckering parameters[12] are Q_T = 0.786(2) Å, ϕ = 11.3(1)°, ϑ = 66.5(1)°for ring C1-C2-C3-C4-C5-N2, and Q_T = 0.669(2) Å, ϕ = 157(1)°, ϑ = 121.2(1)°for ring C1-C2-C3-C6-C7-N1. The two pyridines are twisted with respect to each other, and form a dihedral angle of 30.4(1)°. As previously hypothesized, the *N*-phenylethyl residue does not influence the chiral space around the metal-chelating center.

The complex **4b-CuCl** was also investigated by computational methods, as previously described. Three different conformers, resulting from free rotation of the N1-C12 bond, were studied by means of DFT energy optimization. The conformer found to be the most stable is in accordance with the solid-state structure, as shown by the rmsd value of 0.131 Å (calculated superimposing the heavy atoms of the two structures, Figure 6). The phenyl group is forced toward the *exo* position by the high steric hindrance of the coordinated metal cation, too far from the reacting catalytic center to efficiently induce the enantioselection in the transition state: this finding is in agreement with the experimental outcomes.

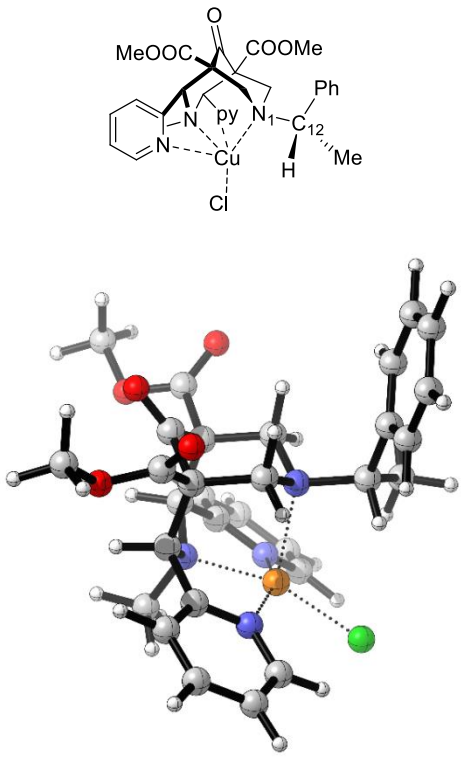

Figure 6: Lowest energy conformer for complex **4b-CuCl**.

Finally, to gather more information on solution phase behaviour of the ligands, ligand-zinc complex solutions, as obtained after the NMR titration, were submitted to ESI analysis (electrospray ionisation mass spectrometry, samples were diluted with acetonitrile, see ESI-MS spectra in the supplementary materials). In these conditions for most of the ligands no peak ascribable to the metal complex was observed, instead only the $[M-H]^+$ signal was detected. A stable

complex ion was instead observed for tetradentate ligand **4b** and pentadentate ligand **4c**. Different species could be detected, resulting from the *in situ* formation of adducts with water or CD_3OH at the carbonyl group. The hydrated **$[L{\cdot}ZnNO_3]^+$** cation (*m/z* = 672.2 for **4b** and *m/z* = 765.2 for **4c**) was observed in both cases. Notably, for ligand **4c**, the base peak was at *m/z* = 719.5. This peak was ascribed to deprotonation of the carbamate nitrogen during the complex formation thus yielding an adduct between the **4c** anion, Zn^{2+} and CD_3OH (the same complexes resulting from the original carbonyl ligand and the adduct with water were also present in the ESI spectrum).

Conclusions

Bispidines are efficient coordinating agents for a number of different metal cations, and the substituents present on their [3.3.1]-diazabicyclo core can have a high impact on their properties as ligands. Experimental catalytic studies of the Henry reactions with benzaldehyde using chiral C_1-symmetric bispidinc ligands have shown that C_2-symmetry is not mandatory to obtain high levels of enantioselectivity. To gain an insight into these different systems, outcomes from structural, spectroscopic and computational techniques were compared and a good agreement between the experimental and the theoretical calculations was observed. As expected, the presence of two pyridine rings strongly stabilizes the formation of a highly stable complex both in solution and in the solid state, while, with simpler bispidines, less stable complexes are formed. The presence of bulky aromatic substituents on the byciclic moiety seems to completely prevent the complexation, whereas chiral residues on the nitrogen atoms are well-tolerated, allowing the formation of quite stable complexes. Several conformational changes occur when moving from the solid state to the solution phase and from the free ligand to the coordinated molecule. This pronounced conformational flexibility can be a drawback for an enantioselective catalysis, where a more rigid catalytic complex, able to efficiently promote a chiral transfer to the transition state, would be preferable. The design of new chiral bispidine catalysts should take into account all these features. Thus, the work presented here could help the forthcoming design of tailored catalytic systems for the Henry reaction.

Experimental

General remarks

All reagents and solvents were purchased from commercial sources and used without further purification. The reactions were carried out under atmospheric air unless otherwise indicated, such as moisture-sensitive ones, for which a static nitrogen atmosphere was used. Reactions were monitored mostly by thin-layer chromatography (TLC), performed on Merck Kieselgel 60 F254 plates. Visualization was accomplished by UV irradiation at 254 nm and subsequently by treatment with alkaline $KMnO_4$ reactant or with phosphomolibdic reagent. Each compound has been purified by silica gel column chromatography (230-400 mesh). ^1H and ^{13}C NMR spectra were recorded on a Bruker 400 spectrometer (^1H NMR, 400 MHz; ^{13}C NMR, 100 MHz). Spectra are registered at room temperature, otherwise indicated, in $CDCl_3$, with tetramethylsilane (TMS, δ=0.0 ppm) used as internal standard. Chemical shifts are reported as δ values in parts per million (ppm) in comparison to internal standards; the coupling constants *J* are reported in Hz. The enantiomeric excess values were determined by chiral HPLC equipped with a DAICEL CHIRAL PAK AD column, according to the following conditions: eluent 9:1, hexane:isopropanol, flow rate 0,75µl/min. ESI-MS spectra were recorded on a Bruker ESQUIRE 3000 PLUS spectrometer, whereas high-resolution mass spectra were recorded on a FT-ICR (Fourier Transform Ion Cyclotron Resonance), equipped with an ESI detector. Optical rotations were determined at 20°C on a Jasco-DIP-181 digital polarimeter (at 589 nm).

Synthetic procedures

Compounds **1a,b**,[6c] **2a**,[6e] **4a,b**[10] were prepared according to literature procedures.

3-methyl-7-((*S*)-1,2,3,4-tetrahydronaphthalen-1-yl)-3,7-diazabicyclo[3.3.1]nonan-9-one (1c). A suspension of (*S*)-1,2,3,4-tetrahydronaphthalen-1-amine (1.45 mL, 0.01 mol), acetic acid (0.57 mL, 0.01 mol), concentrated HCl (0.42 mL, 0.005 mol) and paraformaldehyde (0.63 g, 0.021 mol) in MeOH (10 mL) was stirred for 5 min at 65°C. To this was added dropwise a solution of *N*-

methylpiperidin-4-one (1.23mL, 0.01 mol) and acetic acid (0.57 mL, 0.01 mol) in MeOH (10 mL) over 1 h. After stirring for 10 h the mixture was concentrated in vacuo and the residue was dissolved in water (50 ml). The aqueous phase was washed with diethyl ether (2 x 50 mL) and made strongly basic with 20% KOH solution under ice bath cooling. After extraction with DCM (4 x 100 mL), drying the combined organic layers over Na_2SO_4 and evaporation of the solvent, the residue (orange oil) was purified by silica gel chromatography (ethyl acetate/hexane 8:2) to afford 1.3 g of product (46% yield). Yellowish solid, m.p. 76°C, ^{1}H NMR (400 MHz, $CDCl_3$) δ: 7.75 (d, 1H, *J* = 7.9 Hz), 7.19 (td, 1H, *J* = 7.9, 7.5, 1.6 Hz), 7.13 (td, 1H, *J* = 7.9, 7.5, 1.6 Hz), 7.05 (dd, 1H, *J* = 7.9, 1.6 Hz), 3.96 – 3.86 (m, 1H), 3.14 – 3.06 (m, 2H), 3.05 – 2.98 (m, 3H), 2.96 – 2.88 (m, 1H), 2.87 – 2.79 (m, 2H), 2.78 – 2.67 (m, 2H), 2.64 – 2.52 (m, 2H), 2.33 (s, 3H), 2.00 – 1.88 (m, 2H), 1.80 – 1.60 (m, 2H). ^{13}C NMR (101 MHz, $CDCl_3$) δ: 214.8, 138.4, 137.6, 128.8, 128.6, 126.5, 125.9, 61.5, 60.5, 60.4, 55.1, 53.4, 47.4, 47.0, 45.1, 29.8, 22.3, 21.7. $[\alpha]^{20}_D$ = 11.2 (c 0.5, $CHCl_3$). ν_{max}(ATR) 2935, 2884, 1731, 1446, 1055. MS (ESI): calculated for $C_{18}H_{24}N_2O$: 284.19; found 284.19.

General procedure for the synthesis of bispidinone 2b,c. To a suspension of paraformaldehyde (4.5 mmol) in 20 mL of methanol, the ketone (1 mmol), amine (2 mmol) and acetic acid (0.3 mL) were added. The mixture was heated at reflux for 5 h. On cooling to room temperature the product precipitated and was collect by filtration. The crude was purified by crystallization with ethanol, or alternatively by silica gel chromatography (ethyl acetate/hexane 9:1) affording the pure bispidinone as a solid.

3,7-bis((*S*)-1-cyclohexylethyl)-1,5-diphenyl-3,7-diazabicyclo[3.3.1]nonan-9-one (2b). 71% yield. Yellowish solid, m.p. 159°C ^{1}H NMR (400 MHz, $CDCl_3$) δ: 7.38 – 7.14 (m, 10H), 3.75 (dd, 2H, *J* = 10.6, 1.5 Hz), 3.48 (dd, 2H, *J* = 10.6, 1.5 Hz), 3.24 (d, 2H, *J* = 10.6 Hz), 3.03 (d, 2H, *J* = 10.6 Hz), 2.50 – 2.36 (m, 4H), 1.84 – 1.57 (m, 12H), 1.42 – 1.12 (m, 8H), 0.98 (d, *J* = 6.7 Hz, 6H). ^{13}C NMR (101 MHz, $CDCl_3$) δ: 211.8, 143.9 (2C), 127.9 (2C), 126.9 (2C), 126.4 (2C), 125.9 (2C), 64.3 (2C), 61.7 (2C), 60.9 (2C), 60.7 (2C), 55.2 (2C), 41.0 (2C), 32.0 (2C), 30.3 (2C), 26.7 (2C), 26.5 (2C), 26.3 (2C), 10.8 (2C). $[\alpha]^{20}_D$ = 4.8 (c 1, $CHCl_3$). ν_{max}(ATR) 2942, 2827, 1726, 1566, 1445, 1396, 1168, 1068. MS (ESI): calculated for $C_{35}H_{48}N_2O$: 512.38; found 284.19.

1,5-diphenyl-3,7-bis((*S*)-1,2,3,4-tetrahydronaphthalen-1-yl)-3,7-diazabicyclo[3.3.1]nonan-9-one (2c). 64% yield. Yellowish solid, m.p. 171°C, ^{1}H NMR (400 MHz, $CDCl_3$) δ: 7.90 (d, 2H, *J* = 7.7 Hz), 7.28 – 7.19 (m, 10H), 7.19 – 7.11 (m, 4H), 7.05 (d, 2H, *J* = 7.7 Hz), 4.16 (t, 2H, *J* = 7.0 Hz), 3.79 (dd, 2H, *J* = 10.4, 1.5 Hz), 3.65 (dd, 2H, *J* = 10.4, 1.5 Hz), 3.27 (d, 2H, *J* = 10.4 Hz), 3.23 (d, 2H, *J* = 10.4 Hz), 2.87 – 2.64 (m, 5H), 2.13 – 1.92 (m, 5H), 1.87 – 1.64 (m, 2H). ^{13}C NMR (101 MHz, $CDCl_3$) δ: 211.5, 143.0 (2C), 138.6 (2C), 137.1 (2C), 129.2 (2C), 128.9 (4C), 127.8 (4C), 127.1 (2C), 126.8 (2C), 126.5 (2C), 125.7 (2C), 62.1 (2C), 61.3 (2C), 60.5 (2C), 55.4 (2C), 29.9 (2C), 22.3 (2C), 21.8 (2C). $[\alpha]^{20}_D$ = 6.6 (c 1, $CHCl_3$). ν_{max}(ATR) 2934, 2841, 2785, 1716, 1462, 1445, 1266, 1178. MS (ESI): calculated for $C_{39}H_{40}N_2O$: 552.31; found 284.19.

Dimethyl 7-((1S,2S)-2-((tert-butoxycarbonyl)amino)cyclohexyl)-3-methyl-9-oxo-2,4-di(pyridin-2-yl)-3,7-diazabicyclo[3.3.1]nonane-1,5-dicarboxylate (4c). To a suspension of paraformaldehyde (225 mg, 7.5 mmol) in 20 mL of methanol, dimethyl 1-methyl-4-oxo-2,6-di(pyridin-2-yl)piperidine-3,5-dicarboxylate[16] (1.15 g, 3 mmol) and tert-butyl ((1*S*,2*S*)-2-aminocyclohexyl)carbamate[17] (640 mg, 3 mmol) were added. The mixture was heated at reflux for 24 h. On cooling to room temperature the product precipitated and was collect by filtration. The crude was purified by by silica gel chromatography (ethyl acetate/hexane 9:1) to afford 0.78 g of product (42% yield). Yellowish solid, m.p.: decomposed on heating. ^{1}H NMR (400 MHz, $CDCl_3$) δ: 8.75 (d, 1H, *J* = 4.1 Hz), 8.60 (br s, 1H), 8.49 (d, 1H, *J* = 4.1 Hz), 7.90 – 7.75 (m, 2H), 7.68 (td, 1H, *J* = 7.7, 1.6 Hz), 7.34 (br d, 1H, *J* = 6.6 Hz), 7.30 – 7.21 (m, 1H), 7.17 (ddd, 1H, *J* = 6.6, 4.1, 1.6 Hz), 4.57 (s, 1H), 4.54 (s, 1H), 3.75 (s, 6H), 3.35-3.24 (m, 2H), 3.19 (d, *J* = 11.5 Hz, 1H), 2.89 (d, *J* = 12.0 Hz, 1H), 2.81 (d, 1H, *J* = 12.0 Hz), 2.40 (t, 1H, *J* = 12.0 Hz), 1.86 (s, 3H), 1.76 (d, *J* = 11.1 Hz, 2H), 1.71-1.54 (m, 2H), 1.25 (s, 9H), 1.24 – 1.00 (m, 4H).^{13}C NMR (101 MHz, $CDCl_3$) δ: 203.3, 168.7, 168.5, 157.7, 157.2, 157.1, 149.9, 149.2, 137.2, 136.7, 124.4, 124.1, 123.1, 122.9, 77.2, 74.5, 73.5, 66.4, 64.1, 62.1, 59.2, 52.4, 52.2, 51.7, 50.8, 43.1, 32.9, 28.6 (3C), 25.7, 24.1 (2C). $[\alpha]^{20}_D$ = 8.2 (c 0.5, $CHCl_3$). ν_{max}(ATR) 2960, 2804, 1737, 1587, 1432, 1259, 1092. MS (ESI): calculated for $C_{33}H_{43}N_2O$: 621.32; found 284.19.

NMR spectra of the other compounds match with published literature.

Crystallographic data

Crystals of **2a** and **4a** were obtained as yellow prisms from an acetone/ethanol 1:1 and acetone/methanol 1:1 solution at room

temperature, respectively. Poor quality crystals of **4b-CuCl** were obtained, after many attempts, as blue platelets from an EtOH/water solution at room temperature, respectively. Intensity data were collected on a Bruker Apex II CCD diffractometer, using graphite-monochromatized Mo-Kα radiation (λ = 0.71073 Å). Intensity data were corrected for Lorentz-polarization effects and for absorption (*SADABS*).[18] The structures were solved by direct methods (*SIR-97*)[19] and completed by iterative cycles of full-matrix least squares refinement on F_o^2 and ΔF synthesis using the *SHELXL-17*[20] program (*WinGX* suite).[21] The hydrogen atoms bonded to carbon were included at geometrically calculated positions and refined using a riding model. U_{iso}(H) were defined as $1{\cdot}2U_{eq}$ of the parent carbon atoms for phenyl and methylene residues and $1{\cdot}5U_{eq}$ of the parent carbon atoms for the methyl group. These data can be obtained free of charge *via* www.ccdc.cam.ac.uk/conts/retrieving.html (or from the Cambridge Crystallographic Data Centre, 12, Union Road, Cambridge CB21EZ, UK; fax: ++44 1223 336 033; or deposit@ccdc.cam.ac.uk). CCDC-1822006 (**2a**), CCDC-1822005 (**4a**) and CCDC-1822007 (**4b-CuCl**) numbers contain the supplementary crystallographic data for this paper.

Crystal data for **2a**: $C_{35}H_{36}N_2O$, M_r = 500.66 g/mol, Orthorhombic, Space group $P2_12_12_1$, a = 10.517(7) Å, b = 11.646(7) Å, c = 22.808(7) Å, V = 2755(1) Å^3, Z = 4, D_{calc} = 1.207 Mg/m^3, F(000) = 1072, R = 0.047 (reflections collected/unique = 8970/7288), *wR2* = 0.065, T = 294(2)K, *GOF* = 1.034. The reflections were collected in the range 1.79° ≤ θ ≤ 31.85° (limiting indices = -15≤h≤15, -16≤k≤16, -33≤l≤33) employing a 0.04 x 0.05 x 0.06 mm crystal. The residual positive and negative electron densities in the final map were 0.249 and –0.211 eÅ^{-3}.

Crystal data for **4a**: $C_{32}H_{32}N_4O_9$, M_r = 616.62 g/mol, Orthorhombic, Space group $P2_12_12_1$, a = 9.764(2) Å, b = 14.740(3) Å, c = 24.007(5) Å, V = 3455(1)Å^3, Z = 4, D_{calc} = 1.185 Mg/m^3, F(000) = 1296, R = 0.039 (reflections collected/unique = 15554/4040), *wR2* = 0.1039, T = 294(2)K, *GOF* = 1.111. The reflections were collected in the range 2.19° ≤ θ ≤ 21.65° (limiting indices = -10≤h≤10, -15≤k≤15, -24≤l≤24) employing a 0.63 x 0.32 x 0.12 mm crystal. The residual positive and negative electron densities in the final map were 0.130 and –0.136 eÅ^{-3}.

Crystal data for **4b-CuCl$_2$**: $C_{30}H_{33}Cl_2Cu_1N_4O_8$, M_r = 712.46 g/mol, Monoclinic, Space group $P2_1/c$ 19.0262(8) Å, b = 12.6963(8) Å, c = 13.6195(8) Å, β = 97.93(1)°, V = 3258.5(3) Å^3, Z = 4, D_{calc} = 1.451 Mg/m^3, F(000) = 1245, R = 0.077 (reflections collected/unique = 2787/1637), *wR2* = 0.1445, T = 293(2)K, *GOF* = 1.054. The reflections were collected in the range 1.08° ≤ θ ≤ 19.49° (limiting indices = -17≤h≤17; -11≤k≤11, -12≤l≤12) employing a 0.55 x 0.22 x 0.02 mm crystal. The residual positive and negative electron densities in the final map were 0.326 and –0.395 eÅ^{-3}.

Computational details

Conformational analysis was performed with the software Spartan'08[22] by means of the "conformer distribution" function, using the Monte-Carlo search method. The MMFF force field *in vacuo* was used for the energy minimization of the found structures. The structures were then clustered according to the default setting of the software (which consists in pruning out higher energy conformers, and keeping a diverse set of the low energy conformers using the RMS-torsion definition of nearness). Full geometry optimization of the first ten conformations was performed with DFT at the B3LYP 6-31G (d) level *in vacuo*. All energies were corrected by adding the ZPE as obtained by frequency calculation at the same level.

Conflicts of interest

There are no conflicts to declare.

Acknowledgements

We thank the University of Milan and the Polytechnic of Milan for financial support.

Notes

Additional supporting information may be found in the online version of this article at the publisher's web-site.

References

1 For recent reviews, see: (a) F. A. Luzio, *Tetrahedron*, 2001, **57**, 915. (b) N. Ono, *The Nitro group in Organic Synthesis*, Wiley-VCH, New York, 2001. (c) D. Seebach, A. K. Beck, T. Mukhopadhyay and E. Thomas, *Helv. Chim. Acta*, 1982, **65**, 1101. (d) M. M. Heravi, V. Zadsirjan, M. Dehghani, N. Hosseintash, *Tetrahedron: Asymmetry*, 2017, **28**, 587.

2 (a) A. Cwik, A. Fuchs, Z. Hell and J. M. Clacens, *Tetrahedron*, 2005, **61**, 4015–4021; (b) I. Kudyba, J. Raczko, Z. U. Lipkowska and J. Jurczak, *Tetrahedron* ,2004, **60**, 4807–4820; (c) H.Xu and C. Wolf, *Chem. Commun.*, 2010, **46**, 8026–8028. (a) R. S. Varma, R. Dahiya and S. Kumar, *Tetrahedron Lett.*, 1997, **38**, 5131–5134; (b) N. Ono, *The Nitro Group in Organic Synthesis*, Wiley-VCH, New York, 2001, pp. 30–69; (c) W. E. Noland, *Chem. Rev.*, 1955, **55**, 137–155.(d) Z.-L. Guo, Y.-Q. Deng, S. Zhong, G. Lu, *Tetrahedron: Asymmetry*, 2011, **22**, 1395.

3 (a) G. Murugavel, P. Sadhu, T. Punniyamurthy, *Chem. Rec.*, 2016, **16**, 1906. (b) E. Chinnaraja, R. Arunachalam, P. S. Subramanian, *ChemistrySelect*, 2016, **1**, 5331. (c) V. Ashokkumar, K. Duraimurugan, A. Siva, *New J. Chem.* 2016, **40**, 7148–7156. (d) N. Ananthi, S. Velmathi, *Indian J. Chem., Sect. B: Org. Chem. Incl. Med. Chem.* 2013, **52B**, 87–108. (e) P. Drabina, L. Harmand, M. Sedlak, *Curr. Org. Synth.* 2014, **11**, 879–888. (f) M. J. Rodig, H. Seo, D. Hirsch-Weil, K. A. Abboud, S. Hong, *Tetrahedron: Asymmetry* 2011, **22,** 1097–1102. (g) F. Ibrahim, N. Jaber, V. Guerineau, A. Hachem, G. Ibrahim, M. Mellah, E. Schulz, *Tetrahedron: Asymmetry* 2013, **24**, 1395–1401.

4 (a) Basi V. Subba Reddy, S. Madhusudana Reddy, S. Manisha, C. Madan, *Tetrahedron: Asymmetry*, 2011, **22**, 530. (b) Z. Kałuża, K. Bielawski, R. Ćwiek, P. Niedziejko, P. Kaliski, *Tetrahedron: Asymmetry*, 2013, **24**, 1435.

5 (a) W. J. Ang, Y. S. Chng, Y. Lam, *RSC Adv.* 2015, **5**, 81415. (b) P. Comba, Y.-M. Lee, W. Nam, A. Waleska, *Chem. Commun.* 2014, **50**, 412. (c) M. Breuning, D. Hein, *Eur. J. Org. Chem.* 2013, **2013**, 7575. (d) Y. Zhang, J. Gao, N. Shi, J. Zhao, *Adv. Mater. Res.* 2012, **396–398**, 1236. (e) P. Comba, M. Maurer, P. Vadivelu, *Inorg. Chem.* 2009, **48**, 10389. (f) P. Comba, C. Haaf, A. Lienke, A. Muruganantham, H. Wadepohl, *Chem. - Eur. J*. 2009, **15**, 10880

6 (a) J. Liu, Z. Yang, X. Liu, Z. Wang, Y. Liu, S. Bai, L. Lin, X. Feng, *Org. Biomol. Chem.* 2009, **7**, 4120–4127. (b) Z. Yang, J. Liu, X. Liu, Z. Wang, X. Feng, Z. Su, C. Hu, *Adv. Synth. Catal.* 2008, **350**, 2001–2006. (c) G. Lesma, T. Pilati, A. Sacchetti, A. Silvani, *Tetrahedron Asymmetry* 2008, **19**, 1363–1366. (d) J. Liu, Z. Yang, Z. Wang, F. Wang, X. Chen, X. Liu, X. Feng, Z. Su, C. Hu, *J. Am. Chem. Soc.* 2008, **130**, 5654–5655. (e) G. Lesma, C. Cattenati, T. Pilati, A. Sacchetti, A. Silvani, *Tetrahedron Asymmetry* 2007, **18**, 659–663. (f) G. Lesma, B. Danieli, D. Passarella, A. Sacchetti, A. Silvani, *Letters in Organic Chemistry* 2006, **3**, 430–436. (g) G. Lesma, B. Danieli, D. Passarella, A. Sacchetti, A. Silvani, *Tetrahedron: Asymmetry* 2003, **14**, 2453–2458. (h) O. Huttenloch, E. Laxman, H. Waldmann, *Chem. Commun.* 2002, 673–675. (i) M. J. Dearden, C. R. Firkin, J.-P. R. Hermet, P. O'Brien, *J. Am. Chem. Soc.* 2002, **124**, 11870–11871. (j) J. Spieler, O. Huttenloch, H. Waldmann, *Eur. J. Org. Chem.* 2000, 391–399.

7 S. J. Canipa, A. Stute, P. O'Brien, *Tetrahedron*, 2014, **70**, 7395.

8 H. Maheswaran, K. L. Prasanth, G. G. Krishna, K. Ravikumar, B. Sridhar, M. L. Kantam, *Chem. Commun.*, 2006, **39**, 4066.

9 D. Scharnagel, A. Müller, F. Prause, M. Eck, J. Goller, W. Milius, M. Breuning, *Chem. Eur. J.*, 2015, **21**, 12488.

10 C. Castellano, A. Sacchetti, F. Meneghetti, *Chirality*, 2016, **28**, 332.

11 A. Roux, A. M. Nonat, J. Brandel, V. Hubscher-Bruder, L. J. Charbonnière, *Inorg. Chem.* 2015, **54**, 4431–4444.

12 D. Cremer, J. A. Pople, *J. Am. Chem. Soc.*, 1975, **97**, 1354.

13 L. J. Farrugia, *J. Appl. Cryst.*, 1999, **32**, 837.

14 E. C. Bridgman, M. M. Doherty, K. A. Ellis, E. A. Homer, T. N. Lashbrook, M. E. Mraz, G. C. Pernesky, E. M. Vreeke, K. D. Oshina, A. G. Oliver*, Acta E*, 2016, **72**, 801-804.

15 (a) H. Börzel, P. Comba, K. S. Hagen, M. Kerscher, H. Pritzkow, M. Schatz, S. Schindler, O. Walter, *Inorg. Chem.*, 2002, **41**, 5440. (b) Z. Baranyai, G. Bombieri, F. Meneghetti, L. Tei, M. Botta, *Inorg. Chimica Acta*, 2009, **362**, 2259.

16 T. Legdali, A. Roux, C. Platas-Iglesias, F. Camerel, A. M. Nonat, L. J. Charbonnière, *J. Org. Chem.* 2012, **77**, 11167–11176.

17 P. D. Garimella, A. Datta, D. W. Romanini, K. N. Raymond, M. B. Francis, *J. Am. Chem. Soc.* 2011, **133**, 14704–14709.

18 G. M. Sheldrick, *SADABS Area-Detector Absorption Correction Program*, Bruker AXS Inc., Madison, WI, USA, 2000.

19 A. Altomare; M. C. Burla, M. Camalli, G. L. Cascarano, C. Giacovazzo, A. Guagliardi, A. G. G. Moliterni, G. Polidori, R. Spagna, *J. Appl. Cryst.*, 1999, **32**, 115.

20 G. M. Sheldrick, *SHELX2017 Programs for crystal structure determination*. Universität Göttingen, Germany, 2017.

21 L. J. Farrugia, *J. Appl. Cryst.*, 2012, **45**, 849.

22 Spartan'08, Wavefunction Inc, C.A. Irvine, Y. Shao, L.F. Molnar, Y. Jung, J. Kussmann, C. Ochsenfeld, S.T. Brown, A.T.B. Gilbert, L.V. Slipchenko, S.V. Levchenko, D.P. O'Neill, R.A. Jr DiStasio, R.C. Lochan, T. Wang, G.J.O. Beran, N.A. Besley, J.M. Herbert, C.Y. Lin, T. Van Voorhis, S.H. Chien, A. Sodt, R.P. Steele, V.A. Rassolov, P.E. Maslen, P.P. Korambath, R.D. Adamson, B. Austin, J. Baker, E.F.C. Byrd, H. Dachsel, R.J. Doerksen, A. Dreuw, B.D. Dunietz, A.D. Dutoi, T.R. Furlani, S.R. Gwaltney, A. Heyden, S. Hirata, C-P Hsu, G. Kedziora, R.Z. Khalliulin, P. Klunzinger, A.M. Lee, M.S. Lee, W.Z. Liang, I. Lotan, N. Nair, B. Peters, E.I. Proynov, P.A. Pieniazek, Y.M. Rhee, J. Ritchie, E. Rosta, C.D. Sherrill, A.C. Simmonett, J.E. Subotnik, H.L. Woodcock III, W. Zhang, A.T. Bell, A.K. Chakraborty, D.M. Chipman, F.J. Keil, A. Warshel, W.J. Hehre, H.F. Schaefer, J. Kong, A.I. Krylov, P.M.W. Gill, M. Head-Gordon. Phys Chem Chem Phys 2006, **8**, 3172–3191.